Medium induced jet absorption in relativistic heavy ion collisions

Axel Drees,[1] Haidong Feng,[1] and Jiangyong Jia[1,2]

[1] *Department of Physics and Astronomy, State University of New York, Stony Brook, NY 11794-3800*
[2] *Current Address: Columbia University, New York, NY 10027 and Nevis Laboratories, Irvington, NY 10533, USA*

(Dated: February 8, 2008)

The dense medium created in Au + Au collisions at the Relativistic Heavy-Ion Collider (RHIC) significantly suppresses particle production from hard scattering processes and their characteristic back-to-back angular correlation. We present a simple model of jet absorption in dense matter which incorporates a realistic nuclear geometry. Our calculations are performed at the jet level and assume independent jet fragmentation in the vacuum. This model describes quantitatively the centrality dependence of the observed suppression of the high p_T hadron yield and of the back-to-back angular correlations. The azimuthal anisotropy of high p_T particle production can not be accounted for using a realistic nuclear geometry.

PACS numbers: 27.75.-q

arXiv:nucl-th/0310044v3 31 May 2005

I. INTRODUCTION

In relativistic heavy ion collisions at $62.4 < \sqrt{s_{NN}} < 200$ GeV in the Relativistic Heavy-Ion Collider (RHIC), partons scattered with large Q^2 become a valuable tool to study nuclear matter under extreme conditions. Due to the large Q^2, the hard scattering occurs early in the collisions, thus the scattered partons may directly probe the subsequently produced hot, dense and strongly interacting medium.

In collisions of elementary particles, i.e. in the absence of a dense medium, the hard scattered partons typically fragment into two back-to-back jets of hadrons. These hadrons have large transverse momentum (p_T) and pronounced azimuthal angular correlations. The production cross sections can be calculated with perturbative QCD (pQCD) based on the fragmentation theorem and extrapolated to heavy ion collisions. Theoretical studies predict that the hard scattered partons suffer a large energy loss by multiple scattering and induced gluon radiation as they propagate through dense matter [1]. Unlike energy loss in QED, the radiative gluon energy loss per unit length dE/dx not only depends on the color charge density and the momentum distribution of the partons in the medium, but also linearly depends on the thickness of the medium, due to the non-Abelian nature of gluon radiation in QCD [2, 3].

Data from Au + Au collisions at $\sqrt{s_{NN}} = 130$ and 200 GeV have revealed rich information on high p_T phenomena. One of the most interesting results is the apparent "jet quenching" in central collisions, observed as suppression of the hadron yield by a factor of 4–5 [4, 5, 6] and hadron back-to-back correlation strength by a factor of 5–10 [7], compared to expectations based on the underlying nucleon-nucleon collisions. The absence of these phenomena in d + Au collisions suggests that the observed suppression in central Au + Au collisions is indeed an effect of the dense medium created during the collisions, consistent with parton energy loss in the dense medium [8, 9, 10, 11].

Both the suppression of the high p_T hadron yield and the back-to-back angular correlations show a characteristic centrality dependence, which seems to be independent of p_T for $p_T > 4.5$ GeV/c [4, 5, 6]. Interestingly, in this p_T range, particle production seems consistent with jet fragmentation, despite the suppression. Specifically, experiments have observed:

1. An identical spectral shape compared to $p + p$ collisions within systematic errors [5, 6].
2. A similar suppression for charged hadrons and π^0's [5] and for charged hadron, Λ, and K^0_s [12].
3. A h/π^0 ratio consistent with values observed in $p + p$ collisions, indicating a similar particle composition in $p + p$ and Au + Au at high p_T [5, 13].
4. Strength, width, and charge composition of near angle correlation consistent with jet fragmentation [7].
5. x_T scaling of pion production cross section in Au + Au between $\sqrt{s_{NN}} = 130$ and 200 GeV is similar to $p + p$ collisions [5].

The data suggest that high p_T particles come dominantly from jet fragmentation in vacuum.

In relativistic heavy-ion collisions, energy is deposited in the overlap region between two colliding nuclei. The size, shape and energy density of the medium formed in this region strongly depends on the impact parameter of the collision. The amount of medium a hard scattered parton traverses, and subsequently its energy loss, varies with the centrality of the collision and also the azimuthal angle with respect to the reaction plane. If the parton energy loss is large, the surviving partons will be emitted dominantly near the outer layer of the overlap region [14]. The partons moving towards the surface (near side) traverse on average less material than those going in opposite direction (away side). Thus partons scattered to the near side are likely to escape with little energy loss, while the away side partons are likely to lose significant energy and thus are suppressed more strongly.

It was shown before [15, 16, 17, 18] that for a static non-Abelian partonic medium, the mean total energy loss depends quadratically on the medium size. In addition, the 'dynamical scaling law' allows to write the parton energy loss for an expanding medium in terms of an equivalent static medium with a linear dependence on the path length [17]. Thus to the first order, one can decouple details of the energy loss formulation, which is complicated and model dependent, from the simple geometry of the medium. Recently, several authors have modelled the energy loss of hard scattered partons in Au + Au collisions [19, 20, 21, 22, 23, 24]. Different theoretical approaches for the energy loss have been used and compared to experimental data like the nuclear modification factor R_{AA}, the back-to-back jet correlation strength, and the azimuthal anisotropy of particle production v_2. In general, reasonable agreement between the model calculations and experimental data can be achieved.

In this paper, we present a simple model of jet absorption in an extremely opaque medium, following the approach in Ref. [25] that was used to set a limit on the expected azimuthal anisotropy due to jet quenching. The model is equivalent to an extreme jet energy loss scenario in which most of the energy is lost in a single scattering. We use this simplified model to focus on the geometric aspect of the jet propagation in dense medium. After incorporating a realistic nuclear geometry, we demonstrate that the centrality dependence of the high p_T suppression of the yield and of the back-to-back correlation strength can be described quantitatively. We also discuss the sensitivity of our results on the jet absorption patterns and different collision geometry assumptions, and make predictions for the system size dependence.

II. COLLISION GEOMETRY AND JET ABSORPTION: THE MODEL

Our discussion is limited to centrality dependence of the suppression pattern over the p_T range of 4.5 to 10 GeV/c, where the hadron suppression is approximately constant [5]. Throughout the discussion, the average suppression values for each centrality bin from the data are used to compare with our calculation. Furthermore, since hadron production in this p_T region seems to be consistent with vacuum jet fragmentation, we neglect the medium modification of jet fragmentation and assume that the suppression for partons is identical to the one observed for hadrons[1].

[1] Due to the steeply falling power-law spectra of scattered partons, the hadron p_T spectra is dominated by fragments biased towards large z. As was shown in Ref.[26], the shape of the hadron spectra becomes nearly identical to the shape of the parton spectra, independent of the fragmentation process. Since we model jet absorption at the parton level, the suppression of hadrons thus should be approximately the same as the suppression of partons.

The collision geometry is modelled by a Monte Carlo simulation of Au + Au collisions based on the Glauber approach [27]. For the Au nucleus a Woods-Saxon density distribution with radius $R = 6.38$ fm and diffusivity $a = 0.53$ fm is used [28]. We calculate for each simulated Au + Au collision the underlying number of nucleon-nucleon collisions ($N_{\rm coll}$) and the number of participating nucleons ($N_{\rm part}$), assuming the inelastic nucleon-nucleon cross section is $\sigma_{NN}^{\rm inel} = 42$ mb.

Centrality classes are defined from the fractional cross section by cutting on the impact parameter of the collisions. However, the centrality determination is insensitive to the specific cuts and consequently methods employed elsewhere [29, 30, 31] give similar results. The average number of participants, nucleon-nucleon collisions and impact parameter for different centrality classes are listed in Table. I. For each centrality class, we also calculate the participant density profile, $\rho_{\rm part}(x,y)$, and the nucleon-nucleon collision density profile, $\rho_{\rm coll}(x,y)$, in the plane transverse to the beam direction. The density profiles for a central event class and a peripheral class are shown in Fig. 1; the peak values of the collision and participant densities are also listed in Table I for all centrality classes.

In the following we assume that the energy density is proportional to the participant density. This is motivated by the recognition that the bulk particle production scales approximately with the number of participants [30, 32, 33, 34]. In a later section we study the sensitivity of our results on this assumption. To give the participant density a physical scale we relate it to the energy density using the Bjorken estimate [35],

$$\epsilon_{\rm bj} = \frac{E}{\tau_0 A} \propto \frac{N_{\rm part}}{\tau_0 \pi r_0^2 \left(\frac{N_{\rm part}}{2}\right)^{2/3}} \qquad (1)$$

where $\tau_0 = 0.2 - 1$ fm/c is the formation time, $r_0 = 1.2$ fm is the effective nucleon radius, and $N_{\rm part}$ is the number of participating nucleons. For central collisions the experimentally determined value of $\epsilon_{\rm bj}$ is ≈ 5 GeV/fm^3 [36] for $\tau_0 = 1$ fm/c. With approximately 350 participants the scale factor to convert participant density to $\epsilon_{\rm bj}$ is 2 GeV/fm for $\tau_0 = 1$ fm/c or 10 GeV/fm for $\tau_0 = 0.2$ fm/c.

Binary scaling of hard scattering assumes that the incoming parton distribution in Au + Au collisions is a superposition of the individual nucleon parton distribution functions. According to the factorization theorem the probability for the hard scattering processes in Au + Au is then proportional to $\rho_{\rm coll}$. Therefore we generate back-to-back parton pairs in the transverse plane with a distribution of $\rho_{\rm coll}(x,y)$ and isotropically in azimuth. These partons are then propagated through the nuclear medium with density proportional to $\rho_{\rm part}(x,y)$. The survival probability of a parton produced at (x,y) along direction (n_x,n_y) is calculated as [25]

$$f = \exp(-\kappa I) \qquad , \qquad (2)$$

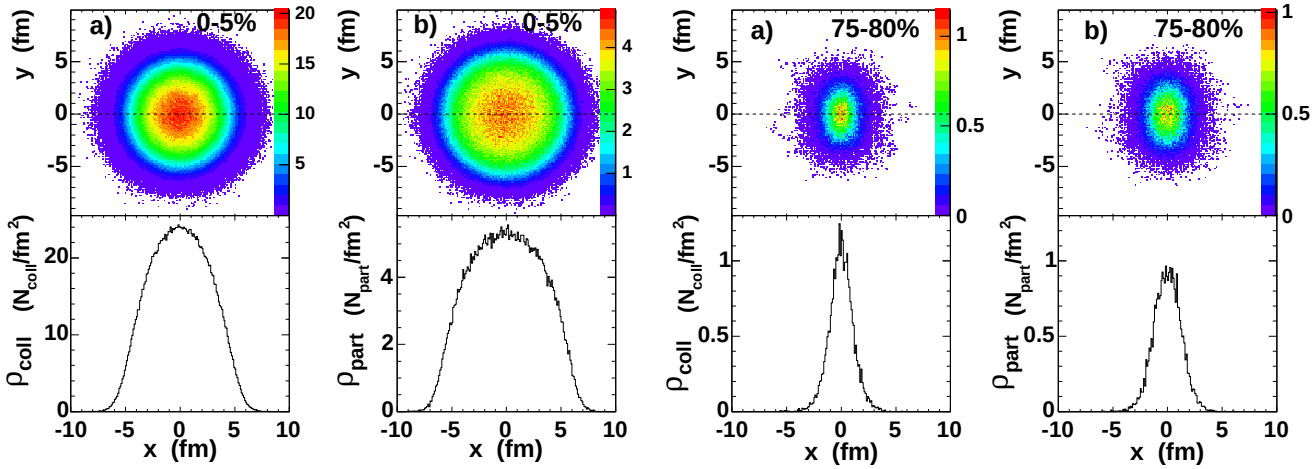

FIG. 1: (Color online) Collision density $\rho_{\rm coll}(x,y)$ (a) and participant density $\rho_{\rm part}(x,y)$ (b) in transverse plane for central (0–5%) and peripheral (75–80%) collisions. The bottom panels are the average density along the impact parameter axis, which is indicated by the dashed line in the top panels.

TABLE I: . Centrality dependence of parameters calculated with a Monte Carlo based Glauber approach. For each centrality class, we list the average number of participants, the average number of nucleon-nucleon collisions, the average impact parameter, the average participant density in the overlap region, the maximum participant density, the maximum nucleon-nucleon collision density, the maximum energy density calculated using the Bjorken estimate at $\tau_0 = 1$ fm/c(see text), and the transverse area with a density larger than 1 GeV/fm^3.

Centrality	$\langle N_{\rm part}\rangle$	$\langle N_{\rm coll}\rangle$	$\langle b\rangle$ (fm)	$\langle\rho_{\rm part}\rangle$ (fm^{-2})	$\rho_{\rm part}^{\rm max}$ (fm^{-2})	$\rho_{\rm coll}^{\rm max}$ (fm^{-2})	$\epsilon_{\rm bj}^{\rm max}$ (GeV/fm^3) ($\tau_0 = 1.0$ fm/c)	$A\left(\epsilon_{\rm bj} > 1\right)$ (fm^2)
0–5%	350	1090	2.2	2.48	4.2	18.9	8.5	138
15–20%	215	540	6.2	2.10	3.8	15.0	7.6	94.7
30–35%	125	250	8.5	1.76	3.1	10.3	6.3	64.7
45–50%	67	105	10.2	1.42	2.4	6.2	4.9	41.6
60–65%	30	35	11.7	1.09	1.5	2.7	3.1	23.2
75–80%	11	10	13	0.79	0.76	0.9	1.5	6.9
90–95%	4.1	2.8	14.5	0.56	0.3	0.23	0.6	0

where κ is the absorption strength, which is the only free parameter in the model. I is the matter integral along the path of the parton, which is calculated as,

$$I = \int_0^\infty dl \;\; l\frac{l_0}{l+l_0}\rho(x+(l+l_0)\,n_x, y+(l+l_0)\,n_y) \quad (3)$$

This parameterization corresponds to a quadratic dependence of the absorption ($\propto ldl$) in a longitudinally expanding medium ($\frac{l_0}{l+l_0}$) [2] . Here we assume that partons travel with speed of the light and that they sense the dense matter after a formation time of 0.2 fm/c or a distance of $l_0 = 0.2$ fm. However, the results presented in this paper do not depend strongly on the choice of l_0.

The absorption strength κ is then fixed in central Au + Au collisions to reproduce the observed hadron suppression. In the following, we use $\kappa = 0.7$ which gives a suppression factor of 4.35 as measured for 0–5% most central collisions by PHENIX [5]. This corresponds to an absorption length of $\lambda \sim 3.4$ fm for a parton traversing an expanding medium with a constant participant density of 2.48 fm^{-2}.

Fig. 2 shows the origination position (x, y) of the hard-scattering partons that escape the medium in 0–5% most central collisions. The depletion at the center of the overlap region is evident. The origins of the surviving jets are almost uniformly distributed over the collision region, which biases jet emission towards the surface of the collision region. Partons emitted from the center of the collision region typically traverse matter with density of more than one participant per fm^2 for a distance of $\gtrsim 5$ fm and thus are frequently absorbed, while partons generated near the surface can easily escape if emitted towards the surface. Therefore, the short absorption length (less than half of the radius of the nuclear overlap) naturally leads to emission of jets and thus of high p_T hadrons from

[2] The effect due to transverse expansion was shown to be small [20].

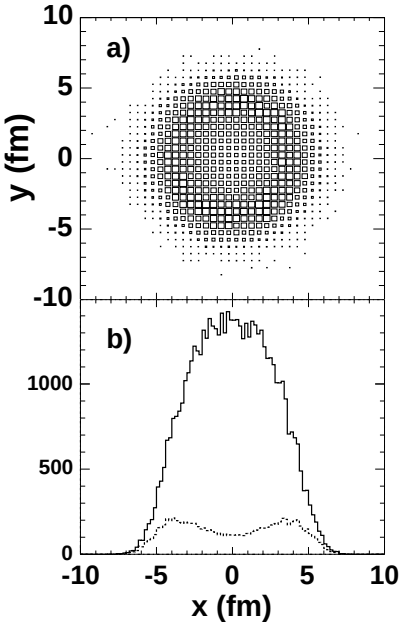

FIG. 2: a) Origination point distribution in the transverse plane for partons escaping the dense medium created in central collisions with $\langle b \rangle \sim 2.2$ fm. b) Generated (solid line) and survived (dotted line) parton initial x position for the cut $|y| < 1$ fm.

outer layer of the medium.

III. CENTRALITY DEPENDENCE OF JET ABSORPTION

Once κ has been determined, the survival rate of jets, the probability to find back-to-back jets, and also the azimuthal anisotropy of emitted jets relative to the reaction plane is fixed for any centrality class. In Fig. 3 we compare our model calculation to the centrality dependence of three compilations of experimental data:

1. Charged hadron and π^0 data from PHENIX [4, 5] and charged hadron data from STAR [6] are plotted on the top panels of Fig. 3. Shown are the ratios of the observed high p_T hadron yields relative to the expected yield from the underlying nucleon-nucleon collisions, normalized to $N_{\rm coll}$, R_{AA} in panel a), or $N_{\rm part}/2$, $R_{AA}^{N_{\rm part}}$ in panel b), of the specific centrality class. The PHENIX data have a lower p_T cut of 4.5 GeV/c, while the STAR data are given for $p_T > 6$ GeV/c.

2. The bottom left panel (c) gives the back-to-back jet correlation strength measured by STAR [7]. The away side correlation strength can be defined by [23]

$$D_{AA}(p_T^{\rm trig}) = \int_{p_0}^{p_T^{\rm trig}} dp_T \int^{|\phi_1-\phi_2|>\phi_0} d\phi \frac{d\sigma_{AA}^{h_1h_2}/d^2p_T^{\rm trig} dp_T d\phi}{d\sigma_{AA}^{h_1}/d^2p_T^{\rm trig}} \quad (4)$$

for an associated hadron h_2 with p_T in backward azimuthal direction of a trigger hadron h_1 with $p_T^{\rm trig}$. The STAR data are for charged trigger particles with $4 < p_T^{\rm trig} < 6$ GeV/c and associated charged hadrons with $p_T > p_0 = 2$ GeV/c detected within $|\phi_1 - \phi_2| > \phi_0 = 2.24$. The data are normalized to the expectation from $p + p$ collisions, and corrected for combinatorial random background and the azimuthal anisotropy of bulk particle production.

3. The azimuthal anisotropy of high p_T charged particles, quantified by v_2, the second Fourier coefficient of the $dN/d\phi$ distribution, is shown in the bottom right panel (d). The PHENIX data are measured for $4 < p_T < 5$ GeV/c with respect to the reaction plane [37]. The preliminary v_2 values from STAR experiment were determined using reaction plane method [38] around 6 GeV/c and 4 particle cumulants for $5 < p_T < 7$ GeV/c [39].

The results of our model calculation are shown as thick solid lines on all panels. Once the absorption strength is adjusted to the observed yield from the most central collisions, the centrality dependence of the normalized yield is well reproduced. In Fig. 3b, the calculated $R_{AA}^{N_{\rm part}}$ increases for peripheral collision, which is expected if the yield scales with the $N_{\rm coll}$ (thin solid line). Only a small fraction of the partons is absorbed since the matter density and volume are small. As the centrality increases both matter density and volume increase; for collisions with more than 100 participants absorption overwhelms the increase due to point like scaling and the $R_{AA}^{N_{\rm part}}$ decreases with centrality.

The jet absorption model also reproduces the magnitude and centrality dependence of the back-to-back correlations without further adjustments. The calculated suppression is negligible for peripheral collisions, increases continuously and reaches a suppression factor of 7 for the most central bin, consistent with the data within errors[3]. The model suggests that the suppression of back-to-back correlations is almost a factor of 1.6 stronger than that for the single inclusive hadron yield. In the jet absorption model, most of the surviving partons come from near the surface of the overlap region. Thus their partner partons have to traverse on average a longer distance through the

[3] We notice, however, due to the large errors of the STAR data, the suppress factor for central collisions is not well constrained.

medium. This naturally leads to a stronger suppression of the back-to-back correlation. It should be noted that in our model, we assume that the jet fragments outside of the medium, in other words, the fragmentation is identical to $p + p$ by construction. Therefore, the near angle jet correlation strength can not deviate from unity in our model.

Due to the asymmetry of the overlap region of the two nuclei, the average amount of matter traversed by a parton depends on its azimuthal direction with respect to the reaction plane, which leads to an azimuthal anisotropy of the emitted jets [19]. This anisotropy reaches its maximum for collisions with an impact parameter of about 9 fm corresponding to approximately 100 participants. It is small for peripheral and central collisions. Our calculation reproduces the measured trend of the centrality dependence of v_2, but the magnitude is below the measured value [4]. With a matter density profile deduced from a Woods-Saxon distribution, a large fraction of the surviving jets is emitted from the low density region at large radii (see Fig. 2b). Therefore the anisotropy is diluted. Larger values of v_2 are obtained for larger κ, but these reproduce neither the suppression of the yield nor the back-to-back correlation strength. For a Woods-Saxon nuclear profile, v_2 reaches a maximum at a certain κ (for $b = 9$ fm, $v_2^{\max} = 10\%$), but then decrease to 0 as $\kappa \to \infty$ because all surviving jets come from the diffuse outer layer of the overlap region, which is essentially isotropic [24]. The calculated v_2 values are very sensitive to the actual nuclear profile used, we shall come back to this in Section IV B.

IV. DISCUSSIONS

A. Dependence on Absorption Pattern

Parton energy loss through gluon bremsstrahlung is thought to be proportional to the path length squared in a static medium [2, 3]. This motivated our ansatz in Eq. 3. We note that although I calculated from Eq. 3 was interpreted as absorption $\propto l^2$ in a longitudinally expanding medium it can also be treated as absorption $\propto l$ in a static medium when l_0 is small. In the following, we denote it as I_1. In order to test the sensitivity of the data to discriminate between different types of energy loss we repeat the calculation for two additional types of absorption,

$$I_2 \;=\; \int_0^\infty dl \;\; \frac{l_0}{l+l_0}\rho(x+(l+l_0)\,n_x, y+(l+l_0)\,n_y)$$

$$I_3 \;=\; \int_0^\infty dl \;\; l\rho(x+ln_x, y+ln_y) \qquad (5)$$

I_2 assumes absorption proportional to the path length l in a longitudinally expanding medium as one may expect for a hadronic energy loss [40] scenario; I_3 assumes a static source and absorption $\propto l^2$. Again the absorption strength is adjusted to give a factor of 4.35 suppression of the yield for central collisions. We find $\kappa = 0.84$ fm ($\lambda = 1.9$ fm) and $\kappa = 0.06$ ($\lambda = 3.6$ fm) for I_2 and I_3, respectively.

The results are compared with each other in Fig. 4. The centrality dependence of the normalized yield is similar for the three different absorption patterns and thus gives little discrimination power. The correlation strength D_{AA} is more sensitive, but the largest sensitivity is found for the anisotropy parameter v_2. The I_2 scenario tends to localize the absorption in the region within the distance of $\approx l_0$ from the jet creation point. In this case, the suppression is dominated by the initial matter profile and is insensitive to the later evolution of the system. This naturally leads to a similar value between R_{AA} and D_{AA}. The surviving jets are also emitted more isotropically resulting in a smaller v_2 [5].

On the other hand, the absorption in a static medium with quadratic path length dependence (I_3) has a strong dependence on the jet path. Partons are absorbed along their full trajectory in the medium. Thus both the suppression of the D_{AA} and the value of v_2 depend more strongly on the centrality of the collision. In particular, one observes a stronger centrality dependence of D_{AA} than of the R_{AA} and a larger v_2. Although the magnitude of v_2 is still below the experimental value.

B. Dependence on Density Profile

Motivated by the approximate $N_{\rm part}$ scaling of bulk particle production, we have assumed that the initial energy density created is proportional to the participant density ($\epsilon \propto \rho_{\rm part}$). A closer look at the data reveals that both the transverse energy E_T and particle multiplicity increase faster than linear with $N_{\rm part}$ [29, 33, 41]. In a two component model [42], the additional increase is attributed to (mini)jet production, which should scale with $N_{\rm coll}$. To test the sensitivity of our model to the initial energy density profile, we repeated the calculation assuming that the energy density is proportional to the collision density $\rho_{\rm coll}(x, y)$.

The results of the calculation are presented in Fig. 5. Generally the agreements between the data and the model calculation are equally good for both matter density profiles. In detail the suppression of the inclusive

[4] We note that the 6% v_2 from our calculations corresponds to a factor of 1.3 larger jet survival probability in reaction plane than out of plane.

[5] In this analysis, we have ignored the transverse expansion, which can further reduce v_2, but only slightly change R_{AA} and D_{AA} [20].

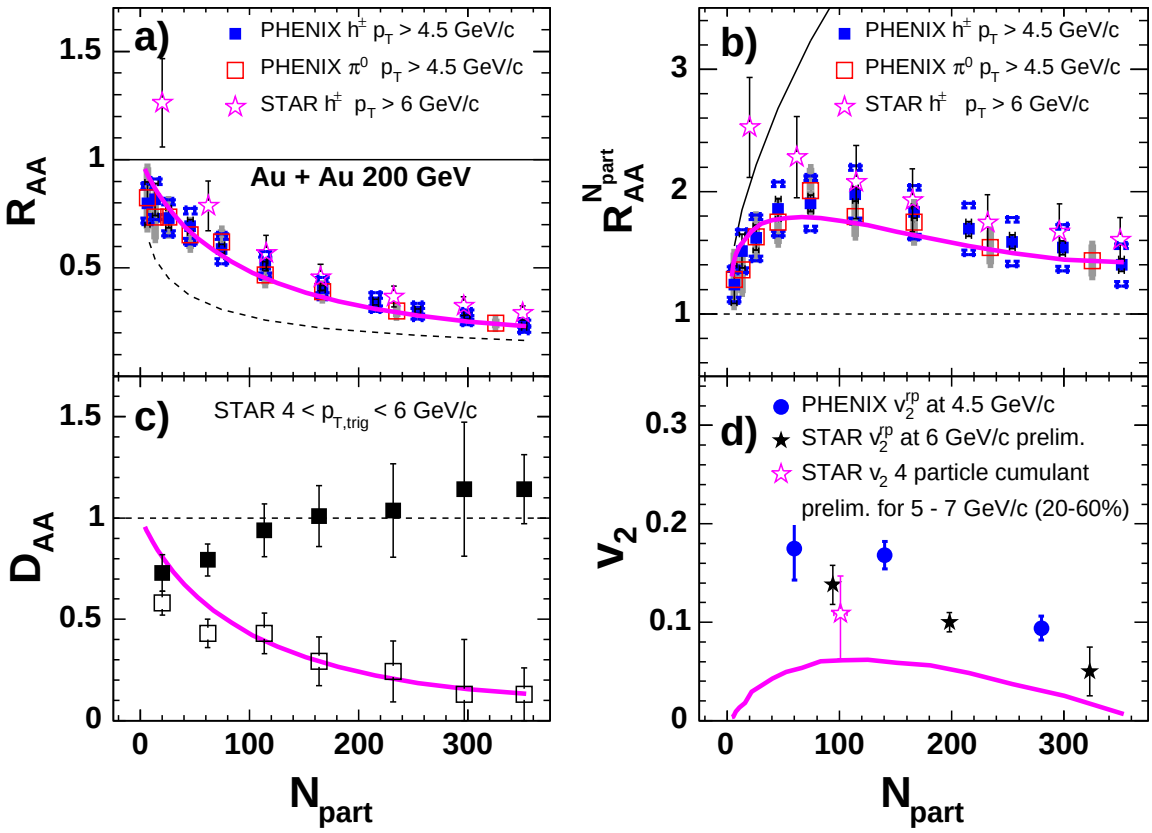

FIG. 3: (Color online) Centrality dependence of normalized yield of high p_T hadrons (a and b), back-to-back correlation strength (c), and v_2 (d) at high p_T. In all four panels, the thick solid line indicates the result of our calculations based on Eqs. 2-3. Further details are discussed in the text.

yield (Fig. 5a and b) shows a slightly stronger centrality dependence. This is easily explained: the absorption strength κ is fixed to reproduce the suppression of the yield in the most central collisions; $\langle \rho_{\rm coll}(x,y) \rangle$ varies by factor of 4 faster than $\left\langle \rho_{\rm part}(x,y) \right\rangle$ from peripheral to central collisions. As a result, the absorption is smaller in peripheral collisions. Similarly D_{AA} is less suppressed in peripheral collisions, but decrease faster for intermediate centralities. On the other hand, the centrality dependence and magnitude of v_2 are similar to Fig. 4, indicating that the two density profiles produce an almost identical anisotropy for all three absorption patterns.

In some recent model calculations nuclear distributions different from a Woods-Saxon profile have been used, typically either a hard-sphere [23, 25] or cylindrical nuclear distributions [21, 43, 44]. The results are significantly different for these unrealistic approximations. In particular, v_2 is increased, where $v_2^{\rm cylindrical} > v_2^{\rm sphere} > v_2^{\rm Woods\text{-}Saxon}$.

Fig. 6 shows the calculations for a hard-sphere nuclear distribution in the top panels and for a cylindrical nuclear distribution in the bottom panels. In both cases, all three absorption scenarios miss the centrality dependence of the normalized inclusive yield. In contrast to the data, the suppression sets in at rather peripheral collisions and remain approximately constant with centrality.

On the other hand, cylindrical and spherical profiles apparently result in much better agreement with v_2 data. The reason is that both cylindrical and hard-sphere collision profiles have sharp surfaces with a large eccentricity, leading to a larger v_2 [45]. In contrast, a Woods-Saxon collision profile has a diffuse surface. While it may be conceivable that the density profile of the matter produced in the collision deviates from the convolution of two Woods-Saxon nuclear distributions, it is hard to imagine that the probability for hard scattering deviates from a Woods-Saxon density distribution significantly.

C. Energy and System Size Dependence

If jet suppression is really dominated by final state energy loss, it should decrease if the energy density or the volume of the medium is reduced. In addition to varying the impact parameter, both volume and density can be reduced by varying the mass number of the colliding nuclei. Alternatively the density may also be changed by varying the beam energy $\sqrt{s_{NN}}$.

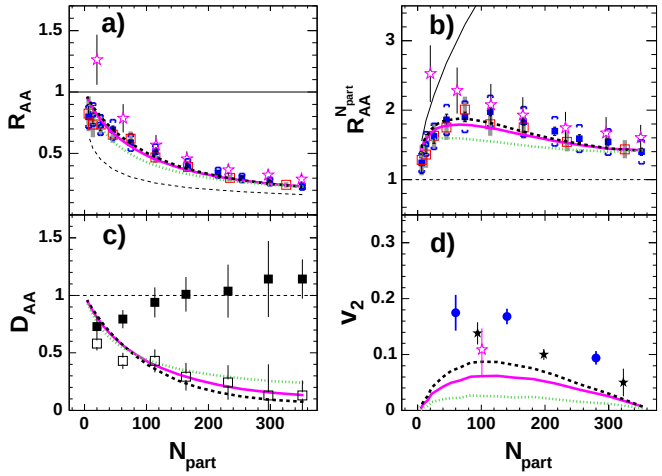

FIG. 4: (Color online) Calculation of R_{AA} (a) $R_{AA}^{N_{\rm part}}$ (b), D_{AA} (c), and v_2 (d) using a Woods-Saxon nuclear profile for I_1 (solid line), I_2 (dotted line), and I_3 (dashed line) types of jet absorption.

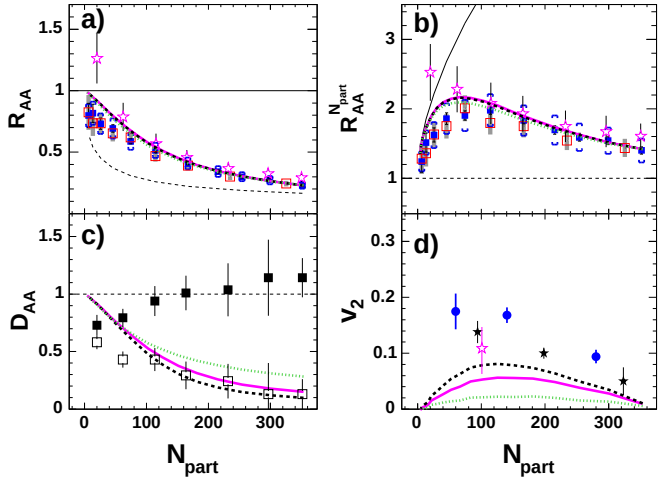

FIG. 5: (Color online) Calculation of R_{AA} (a), $R_{AA}^{N_{\rm part}}$ (b), jet correlation (c), and v_2 (d) assuming $\epsilon \sim \rho_{\rm coll}$. The three curves are for I_1 (solid line), I_2 (dotted line), and I_3 (dashed line) types of jet absorption, respectively.

The jet absorption model can provide a simple baseline prediction for both the beam energy and system size dependence of the suppression, if we assume that the absorption strength κ is the same as in $\sqrt{s_{NN}}$=200 GeV Au + Au collisions. We limit the discussion to the calculation presented in section II.

The system size dependence can be evaluated without further assumptions. In Fig. 7 the nuclear modification factor R_{AA} for central collisions of smaller systems (see Table. II) at $\sqrt{s_{NN}}$=200 GeV is compared to the calculated centrality dependence for Au + Au collisions (see Fig. 3). The agreement of the absolute values and the $N_{\rm part}$ dependence of the R_{AA} and D_{AA} is remarkable. This implies that to the first order the volume is proportional to $N_{\rm part}$ and that the participant densities profiles are very similar. This similarity is illustrated in Fig. 8 by comparing the integral distribution I_1 experienced by the generated partons in central collisions for various collision systems with that for centrality selected Au + Au collisions with similar $N_{\rm part}$. Since the jet correlation strength also depends on the volume and average density, the calculated D_{AA} is also similar for light systems and corresponding Au + Au collisions. In contrast, the anisotropy calculated for central collisions of smaller nuclei is consistent with zero as expected.

To guide our estimate of the beam energy dependence we assume that the matter density scales like the Bjorken energy density. For an average mix of quark and gluon jets which we do not vary with $\sqrt{s}$, we fix the absorption coefficient κ to be the same as in $\sqrt{s_{NN}}$ = 200 GeV. In this estimation the energy density increases by a factor of 2 from SPS ($\sqrt{s_{NN}}$ = 17 GeV) to RHIC ($\sqrt{s_{NN}}$ = 200 GeV) energies. Interpolating between these values and scaling down the density in our calculation accordingly, we find that the high p_T hadron suppression is still a factor ~3 for lower energy RHIC run at $\sqrt{s_{NN}}$ = 62.4 GeV.

Our estimation would also predict a factor of 2 suppression at SPS energies, which is not observed experimentally. However, data at the SPS [46] are limited to p_T below 4 GeV/c, a region where other mechanism like p_T broadening and hydrodynamic flow complicate the interpretation of particle production in heavy ion collisions. We noted that the predictive power of our approach is limited, because we did not take into account the $\sqrt{s_{NN}}$ dependence of the quark (gluon)jet fraction, the hard-scattering cross section and the system lifetime, which could be important.

V. CONCLUSION

We have shown that the experimentally observed centrality dependence of the suppression of the hadron yield R_{AA} and the suppression of back-to-back correlation D_{AA} can be quantitatively described by jet absorption in an opaque medium when a realistic nuclear geometry is included. In our model, the centrality dependence of R_{AA} and of the D_{AA} are rather insensitive to the details of the medium density profile. R_{AA} is also insensitive to the absorption patterns. Both R_{AA} and D_{AA} do not distinguish between central collisions of small systems and centrality selected Au + Au collisions with similar $N_{\rm part}$. Our interpretation is that R_{AA} and D_{AA} depend mostly on volume and average density of the opaque medium. In the limit of very opaque matter, R_{AA} probably will not reveal further insight into the details of the absorption pattern or alternatively of the energy loss and the density profile, unless data at much higher p_T become available.

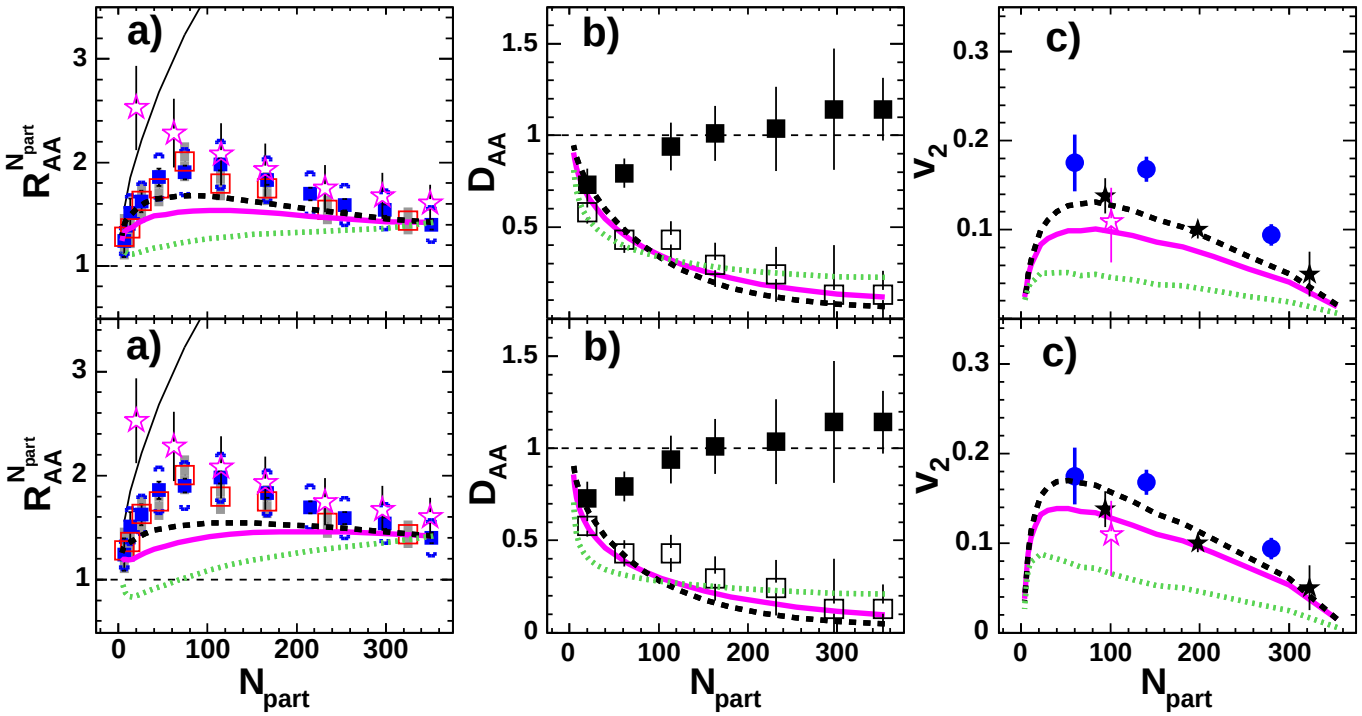

FIG. 6: (Color online) Calculation of $R_{AA}^{N_{\rm part}}$ (a), D_{AA} (b), and v_2 (c) for a hard-sphere nuclear profile (top panels) and a cylindrical nuclear profile (bottom panels) using the I_1 (solid line), I_2 (dotted line), and I_3 (dashed line) form of jet absorption.

TABLE II: List of light collisions systems and corresponding $N_{\rm part}$ for 0–5% central collisions.

Species	O + O	Si + Si	Fe + Fe	Cu + Cu	Zr + Zr	I + I	La + La
$N_{\rm part}$	24	45	95	109	159	224	246

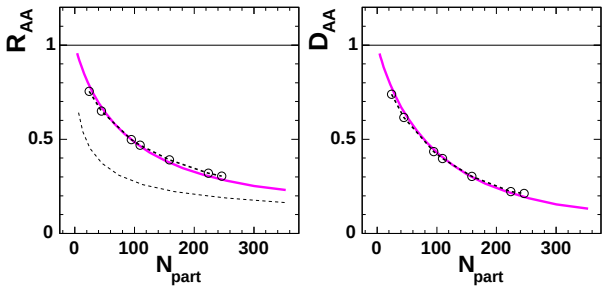

FIG. 7: (Color online) The calculated system size dependence (open circles) of the R_{AA} (left) and D_{AA} (right) compared with their centrality dependence in Au + Au collisions (thick solid line). The open circles are calculated for 0–5% most central collisions for each collision system. The thick solid line represent the calculation for I_1 type of absorption (same calculation shown in Fig. 3b and c.)

We find that observables like D_{AA} and v_2 are more sensitive to the absorption patterns. Our model does not describe v_2 quantitatively unless an unrealistic nuclear density profile is used. This might indicate that the actual diffuseness of the opaque medium is smaller than expected from the density profile obtained by convoluting two Woods-Saxon nuclear distributions [19]. It is also conceivable that the real suppression is larger, and that the observed suppression is reduced by "soft" particles from dynamic mechanisms different from jet fragmentation, such as hydrodynamics [48] plus viscosity correction [49], quark coalescence [47], and quark/diquark pick up [24]. In this case, both the "soft" particles and a stronger suppression would lead to a larger v_2.

Acknowledgments: We greatly appreciate the fruitful discussions with P. Kolb, E. Shuryak, and J.C. Solana. This work was supported by the Department of Energy, Office of Science, and Nuclear Physics Division under Grant No. DE-FG02-96ER40988.

[1] M. Gyulassy and M. Plümer, Phys. Lett. **B 243**, 432 (1990); X.N. Wang and M. Gyulassy, Phys. Rev. **68**, 1480 (1992); R. Baier *et al.*, Phys. Lett. **B 345**, 277 (1995).

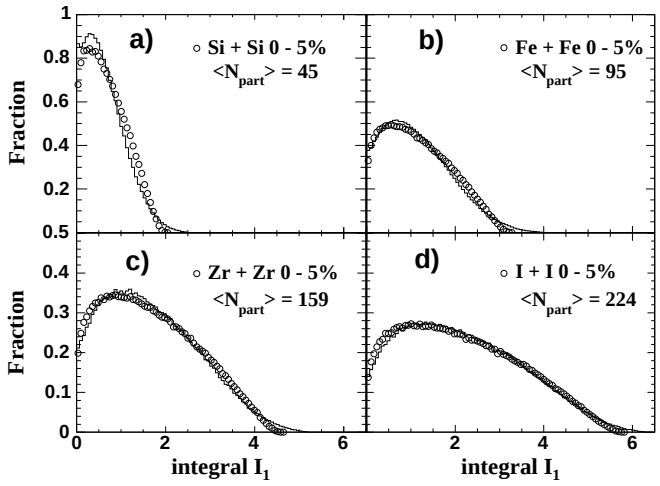

FIG. 8: The matter integral I_1 distributions as defined in Eq. 3 for central a) Si + Si, b) Fe + Fe, c) Zr + Zr, d) I + I collisions (solid circles) compared with Au + Au collisions (solid lines) at different impact parameters with similar $\langle N_{\rm part}\rangle$.

[2] R. Baier, D. Schiff and B.G. Zakharov, Annu. Rev. Nucl. Part. Sci. **50**, 37 (2000).
[3] R. Baier, Y.L. Dokshitzer, A.H. Mueller and D. Schiff, J. High Energy Phys. **09**, 033 (2001)
[4] S.S Adler *et al.*, [PHENIX Collaboration], Phys. Rev. **91**, 072301 (2003).
[5] S.S Adler *et al.*, [PHENIX Collaboration], Phys. Rev. **C 69**, 034910 (2004).
[6] J. Adams *et al.*, [STAR Collaboration], Phys. Rev. **91**, 172302 (2003).
[7] C. Adler *et al.*, [STAR Collaboration], Phys. Rev. **90**, 082302 (2002).
[8] B.B. Back *et al.*, [PHOBOS Collaboration], Phys. Rev. **91**, 072302 (2003).
[9] S.S Adler *et al.*, [PHENIX Collaboration], Phys. Rev. **91**, 072303 (2003).
[10] J. Adams *et al.*, [STAR Collaboration], Phys. Rev. **91**, 072304 (2003).
[11] I. Arsene *et al.*, [BRAHMS Collaboration], Phys. Rev. **91**, 072305 (2003).
[12] J. Adams *et al.*, [STAR Collaboration], Phys. Rev. **92**, 052302 (2004).
[13] S.S Adler *et al.*, [PHENIX Collaboration], Phys. Rev. **91**, 172301 (2003).
[14] J.D. Bjorken, FERMILAB-PUB-82-059-THY (unpublished).
[15] E. Wang and X.N. Wang, Phys. Rev. **87**, 142301 (2001).
[16] M. Gyulassy, P. Levai and I. Vitev, Phys. Rev. **85**, 5535 (2000).
[17] C.A. Salgado and U.A. Wiedemann, Phys. Rev. **89**, 092303 (2002).
[18] R. Baier, Yu.L. Dokshitzer, A.H. Mueller and D. Schiff, Nucl. Phys. **B531**, 403 (1998).
[19] M. Gyulassy, I. Vitev and X.N. Wang, Phys. Rev. **86**, 2537 (2001).
[20] M. Gyulassy, I. Vitev, X.N. Wang and P. Huovinen, Phys. Lett. **B 526**, 301 (2002).
[21] B. Müller, Phys. Rev. **C 67**, 061901 (2003).
[22] T. Hirano and Y. Nara, Phys. Rev. **91**, 082301 (2003).
[23] X.N. Wang, Phys. Lett. **B 595**, 165 (2004).
[24] J.C. Solana and E.V. Shuryak, `hep-ph/0305160`.
[25] E.V. Shuryak, Phys. Rev. **C** 66 027902 (2002).
[26] M. Jacob and P.V. Landshoff, Phys. Repts. **48**, 285 (1978).
[27] R.J. Glauber and G. Matthiae, Nucl. Phys. B **21**, 135 (1970).
[28] B. Hahn, D.G. Ravenhall and R. Hoftstadter, Phys. Repts. **101**, 1131 (1956).
[29] K. Adcox *et al.*, [PHENIX Collaboration], Phys. Rev. **86**, 3500 (2001).
[30] D. Kharzeev and M. Nardi, Phys. Lett. **B 507**, 121 (2001).
[31] C. Adler *et al.*, [STAR Collaboration], Phys. Rev. **89**, 202301 (2002).
[32] A. Bialas, A. Bleszynski and W. Czyz, Nucl. Phys. **B111**, 461 (1976).
[33] A. Bazilevsky, for the PHENIX Collaboration, Nucl. Phys. **A715**, 486 (2003).
[34] NA49 Collaboration, P.G. Jones *et al.*, Nucl. Phys. **A610**, 188 (1996); WA98 Collaboration, T. Peitzmann *et al.*, Nucl. Phys. **A610**, 200 (1996); WA80 Collaboration, R. Albrecht *et al.*, Phys. Rev. **C 44**, 2736 (1998).
[35] J.D. Bjorken, Phys. Rev. **D 27**, 140 (1983).
[36] K. Adcox *et al.*, [PHENIX Collaboration], Phys. Rev. **87**, 052301 (2001).
[37] S.S Adler *et al.*, [PHENIX Collaboration], Phys. Rev. **91**, 182301 (2003) .
[38] K. Filimonov, Nucl. Phys. **A715**, 737 (2003).
[39] R. Snellings, [STAR Collaboration], Heavy Ion Phys. **21**, 237 (2004).
[40] K. Gallmeister, C. Greiner and Z. Xu, Phys. Rev. **C 67**, 044905 (2003).
[41] B.B. Back *et al.*, [PHOBOS Collaboration], Phys. Rev. **C 67**, 021901R (2003).
[42] S. Li and X.N. Wang Phys. Lett. **B 527**, 85 (2002).
[43] D. Kharzeev, E. Levin and L. McLerran, Phys. Lett. **B 561**, 93 (2003) and references therein.
[44] Y.V. Kovchegov and K.L. Tuchin, Nucl. Phys. **A708**, 413 (2002).
[45] S.A. Voloshin, Nucl. Phys. **A715**, 379 (2003).
[46] WA98 Collaboration, M.M. Aggarwal *et al.*, Eur. Phys. J. **C 23**, 225 (2002); CERES Collaboration, G. Agakishiev *et al.*, hep-ex/0003012; NA49 Collaboration, H. Appleshauser, *et al.*, Phys. Rev. **82**, 2471 (1999).
[47] R.C. Hwa and C.B. Yang, Phys. Rev. **C 67**, 034902 (2003); R.J. Fries, B. Muller, C. Nonaka and S.A. Bass, Phys. Rev. **90**, 202303 (2003).
[48] P.F. Kolb and U. Heinz, review for 'Quark Gluon Plasma 3', Editors: R.C. Hwa and X.N. Wang, World Scientific, Singapore, `nucl-th/0305084`.
[49] D. Teaney, `nucl-th/0301099`.